Human Immunology 86 (2025) 111249

Contents lists available at ScienceDirect

journal homepage: www.elsevier.com/locate/humimm

Research article

Convalescent COVID-19 monocytes exhibit altered steady-state gene expression and reduced TLR2, TLR4 and RIG-I induced cytokine expression

Sarah Unterberger [a,1], Nadia Terrazzini [b], Sandra Sacre [a,*]

[a] Brighton and Sussex Medical School, University of Sussex, Brighton, UK
[b] Centre for Regenerative Medicine and Devices, School of Applied Sciences, University of Brighton, Brighton, UK

ARTICLE INFO

Keywords:
COVID-19
RIG-I
Toll-like receptor
Monocytes
SARS-CoV-2
Gene expression

ABSTRACT

Severe acute respiratory syndrome coronavirus 2 (SARS-CoV-2), which causes COVID-19, can induce trained immunity in monocytes. Trained immunity is the result of metabolic and epigenetic reprogramming of progenitor cells leading to an altered inflammatory response to subsequent activation. To investigate the monocyte response 3–6 months post SARS-CoV-2 infection, steady-state gene expression and innate immune receptor stimulation were investigated in monocytes from unvaccinated SARS-CoV-2 naïve individuals and convalescent COVID-19 participants. The differentially expressed genes (DEGs) identified were involved in the regulation of innate immune signalling pathways associated with anti-viral defence. COVID-19 participants who had experienced severe symptoms exhibited a larger number of DEGs than participants that had mild symptoms. Interestingly, genes encoding receptors that recognise SARS-CoV-2 RNA were downregulated. *DDX58,* encoding retinoic-acid inducible gene I (RIG-I), was downregulated which corresponded with a reduced response to RIG-I activation. Furthermore, toll-like receptor (TLR)1/2 and TLR4 activation also exhibited reduced cytokine secretion from convalescent COVID-19 monocytes. These data suggest that following SARS-CoV-2 infection, monocytes exhibit altered steady-state gene expression and reduced responsiveness to innate immune receptor activation. As both RIG-I and TLRs recognise components of SARS-CoV-2, this may lead to a moderated inflammatory response to SARS-CoV-2 reinfection in the months following the initial infection.

1. Introduction

Severe acute respiratory syndrome coronavirus 2 (SARS-CoV-2), that causes Coronavirus disease 2019 (COVID-19), activates the innate immune system upon infection inducing inflammation. During the early waves of COVID-19 in 2020, infected individuals experienced a range of mild to moderate symptoms such as a cough, fever and fatigue. However, about 10% of patients developed more severe inflammation, particularly in the lungs, requiring hospitalisation, oxygen supplementation, or even ventilation. The most critical cases developed acute respiratory distress syndrome, septic shock, multi-organ dysfunction and in some cases, this resulted in death [1–3]. Following the resolution of acute infection, some people develop a condition termed post-acute sequelae of SARS-CoV-2 infection or long COVID. This is characterised by the persistence of symptoms for three months or more [4]. The pathogenesis is unclear, but an association with a persis-

Abbreviations: COVID-19, Coronavirus disease 2019; BCG, Bacille Calmette-Guerin; CBLB, Cbl proto-oncogene B; CXCL, C-X-C motif chemokine ligand; DEGs, Differentially expressed genes; ELISA, Enzyme-linked Immunosorbent assay; FPR1, Formyl peptide receptor 1; GO, Gene ontology; GOI, Gene of interest; HC, Healthy control; IFI, Interferon-γ-inducible; IFIH1, Interferon induced with helicase C domain 1; IFN, Interferon; IL, Interleukin; IRAK, Interleukin-1 receptor-associated kinase; IQR, Interquartile range; JAK, Janus kinase; KEGG, Kyoto Encyclopedia of Genes and Genomes; LPS, Lipopolysaccharide; LILRA3, Leukocyte immunoglobulin like receptor A3; log2FC, Log2 fold change; MAPK, Mitogen-activated protein kinase; MDA5, Melanoma differentiation-association protein 5; MyD88, Myeloid differentiation primary response protein 88; NF, Nuclear factor; NLRP, NOD-like receptor family pyrin domain containing; NOD, Nucleotide-binding oligomerization domain; OAS, Oligoadenylate synthetase; OSM, Oncostatin m; PAM3, PAM3CSK4; PBMCs, Peripheral blood mononuclear cells; qPCR, Quantitative polymerase chain reaction; RIG-I, Retinoic-acid inducible gene I; RT-PCR, Reverse transcription polymerase chain reaction; S100A12, S100 calcium-binding protein A12; SARM1, Sterile α and HEAT/Armadillo motif containing protein 1; SARS-CoV-2, Severe acute respiratory syndrome coronavirus 2; SD, Standard deviation; SIGIRR, Single Ig IL-1-related receptor; SOCS, Suppressor of cytokine signalling; ssRNA, Single-stranded RNA; STAT, Signal transducer and activator of transcription; STRING, Search Tool for the Retrieval of Interacting Genes; TAK, TGF-β-activated kinase; TLR, Toll-like receptor; TNF, Tumour necrosis factor-α; TNFAIP3, TNF-alpha-induced protein 3; TOLLIP, Toll-interacting protein; TRAF, TNF receptor-associated factor.

* Corresponding author at: Brighton and Sussex Medical School, Medical Research Building, University of Sussex, Brighton, East Sussex BN1 9PS, UK.
E-mail address: s.sacre@bsms.ac.uk (S. Sacre).
[1] Present address: Biotech Research & Innovation Centre (BRIC), University of Copenhagen, Copenhagen, Denmark.

https://doi.org/10.1016/j.humimm.2025.111249
Received 23 August 2024; Revised 12 January 2025; Accepted 21 January 2025

tent reservoir of SARS-CoV-2 and/or an induced immune dysregulation have been suggested [5]. Several studies have emerged, indicating that innate immune cells can undergo trained immunity following infection with SARS-CoV-2, leading to sustained epigenetic and metabolic changes [6–8].

Being a positive-sense single-stranded RNA (ssRNA) virus, SARS-CoV-2 is recognized by toll-like receptor (TLR)7, TLR8, retinoic-acid inducible gene I (RIG-I) and melanoma differentiation-associated protein 5 (MDA5) [9–11]. In addition, the SARS-CoV-2 envelope protein can activate TLR2, independent of viral entry or replication [12,13]. Whereas TLR4 on macrophages is activated by the SARS-CoV-2 spike protein S1 subunit, leading to proinflammatory cytokine production [14,15].

Accordingly, circulating monocytes from COVID-19 patients exhibit phenotypic changes, with increased expression of activation markers and production of inflammatory mediators [16,17]. Following exposure to an inflammatory stimulus, monocytes can develop an altered response to further challenge. Short-term changes can be induced, such as immune tolerance following stimulation of TLR4 with lipopolysaccharide (LPS), resulting in reduced cytokine production upon a subsequent challenge due to associated alterations in gene expression [18,19]. However, more long-term changes have also been observed, where monocytes and their progenitor haematopoietic stem cells undergo epigenetic and metabolic reprogramming, leading to a sustained modification in their transcriptional profile, termed trained immunity [20]. For example, after tuberculosis vaccination with Bacille Calmette-Guerin (BCG), monocyte responses to unrelated bacterial and fungal pathogens are increased up to 3 months post vaccination [21]. Similarly, due to COVID-19, monocytes display a prolonged remodelling of chromatin accessibility, suggesting the induction of trained immunity [6,7].

To explore the effect of SARS-CoV-2 infection on the recovery phase 3–6 months after infection, the transcriptional profile of host response genes alongside the responsiveness to TLR1/2, TLR4 and RIG-I activation were investigated. This was performed using monocytes from individuals infected during the first wave of COVID-19 in the UK and compared to monocytes from healthy volunteers that were collected prior to the emergence of SARS-CoV-2 or the administration of COVID-19 vaccines.

2. Materials and Methods

2.1. Study population

This study was approved by the Brighton and Sussex Medical School Research Governance Ethics Committee (ER/BSMS2373/1). COVID-19 participants were recruited 3–6 months following a positive reverse transcription polymerase chain reaction (RT-PCR) for SARS-CoV-2 (oropharyngeal and/or nasal swab) during the first wave of COVID-19 in early 2020. Participants were categorised into two groups based on self-reported disease severity. Individuals who were symptomatic and managed their symptoms at home without requiring hospital care or advanced medical support were classified as mild, whereas those who experienced significant shortness of breath or low oxygen saturation requiring hospitalisation and oxygen supplementation were classified as severe. Further details of the participants' characteristics and symptoms are provided in Table 1. Samples previously collected prior to the emergence of SARS-CoV-2 were included in the study as healthy controls (HC). None of the participants had received a COVID-19 vaccine, as the blood samples were collected prior to these vaccines being administered to the public.

2.2. Isolation and cell culture of primary human monocytes

Peripheral blood mononuclear cells (PBMCs) were isolated from whole venous blood using Ficoll-Paque gradients (Cedarlane, Burlington, Canada) as previously described [22]. Monocytes were then isolated using CD14+ selection beads (Miltenyi Biotec, Cologne,

Table 1
Characteristics of study participants. Data are n (%) except where indicated. SD: standard deviation; IQR: interquartile range.

Characteristics	Value		
Study participants, n	COVID-19 Mild cases (n = 8)	COVID-19 Severe cases (n = 8)	Healthy controls (n = 12)
Age; years, median (IQR)	53 (11.5)	54 (17.5)	46 (22) (3 unknown)
Sex; female:male	5:3	5:3	7:5
Sample collection; days since positive PCR test (SD)	110 (19)	134 (21)	
Underlying health condition	0 (0)	3 (37.5)	
IgG levels against SARS-CoV-2 S1 Spike protein (median (range); μg/ml)	2.22 (0.22–25.34)	22.25 (7.8–30.19)	0.8942 (0.0–0.9744) n = 5
IgM levels against SARS-CoV-2 S1 Spike protein (median (range); μg/ml)	0.65 (0.42–2.12)	3.19 (0.41–12.17)	
Characteristics and symptoms in acute phase of disease			
Duration of acute symptoms (days (SD))	12 (5) (1 unknown)	39 (25) (2 unknown)	
Hospital admission	0 (0)	8 (100)	
Intensive care unit	0 (0)	1 (12.5)	
Oxygen required	0 (0)	8 (100)	
Fever	6 (75)	7 (87.5)	
Cough	5 (62.5)	6 (75)	
Dyspnea	3 (37.5)	8 (100)	
Olfactory and taste dysfunction	5 (62.5)	3 (37.5)	
Fatigue	5 (62.5)	8 (100)	
Abdominal pain	3 (37.5)	5 (62.5)	
Continuous symptoms post recovery	3 (37.5)	5 (62.5)	
Cough	0 (0)	1 (12.5)	
Olfactory and taste dysfunction	1 (12.5)	0 (0)	
Fatigue	1 (12.5)	3 (37.5)	
Dyspnea	1 (12.5)	4 (50)	
Abdominal discomfort	0 (0)	1 (12.5)	

Germany) as per the manufacturer's instructions. For cell stimulations, purified monocytes were cultured at 37°C and 5% CO_2 in RPMI 1640 media containing 5% (v/v) FBS and 100U/ml penicillin/streptomycin. Cells were then stimulated for 24 h with 100ng/ml PAM3CSK4 (PAM3) (Axxora, Nottingham, UK), 10ng/ml LPS (Axxora, Nottingham, UK), or 1μg/ml 3p-hpRNA (Invivogen, Toulouse, France). The transfection of 3p-hpRNA was performed with lyoVec (Invivogen, Toulouse, France) according to the manufacturer's instructions.

2.3. Enzyme-linked Immunosorbent assay (ELISA)

IgG and IgM levels against SARS-CoV-2 S1 Spike protein were tested in sera collected from all of the convalescent participants using Legend Max™ kits (Biolegend, San Diego, CA, USA) following the manufacturer's instructions. Samples were diluted 1:100, 1:1000, 1:10000 for IgG and 1:100, 1:1000 for IgM quantification, before incubation on the ELISA plates. The optical density was read at 450nm on a plate reader (Biotek, Winooski, VT, USA). Standard curves with serial dilutions of S1 IgG (15–0.23 ng/ml range) and IgM (30–0.46 ng/ml range) were used to calculate the concentrations of anti-S1 IgG and IgM.

Sandwich ELISAs were applied to measure interleukin (IL)-1β, IL-6, tumour necrosis factor-α (TNF) and C-X-C motif chemokine ligand (CXCL)10 in cell supernatants. IL-1β capture antibody (MAB601, R&D systems, Abingdon, UK), biotinylated IL-1β antibody (BAF201, R&D systems, Abingdon, UK), IL-6 capture antibody (554543, Becton Dickinson, Oxford, UK), biotinylated IL-6 antibody (554546, Becton Dickinson, Oxford, UK), TNF capture antibody (551220, Becton Dickinson, Oxford, UK), TNF biotinylated antibody (554511, Becton Dickinson, Oxford, UK), CXCL10 capture antibody (555046, Becton Dickinson, Oxford, UK) and biotinylated CXCL10 antibody (BAF266, R&D systems, Abingdon, UK) were used according to the manufacturer's instructions. Recombinant IL-6, TNF, CXCL10 and IL-1β were purchased from PeproTech (London, UK). The IL-1β ELISA detects both pro-IL-1β and mature IL-1β. Streptavidin horseradish peroxidase (DY998, R&D systems, Abingdon, UK) and 3,3′,5,5′-Tetramethylbenzidine microwell peroxidase substrate kit (KPL Inc., Gaithersburg, USA) were used according to the manufacturer's instructions. Colour formation was stopped using 0.16 M sulfuric acid. Absorbance was read at 450 nm on a Biotek synergy HT Microplate reader and analysed using Gen5 software (BioTek, Winooski, VT, USA).

2.4. RNA preparation and NanoString nCounter assay

RNA was extracted using the Rneasy Mini Kit (QIAGEN, Stockach, Germany) according to the manufacturer's instructions. Samples were analysed using the nCounter Human Host Response V1 panel (NanoString Technologies, Inc., Seattle, WA, USA) on a Nanostring nCounter *SPRINT*™ Profiler (NanoString Technologies, Inc., Seattle, WA, USA) according to the manufacturer's instructions. For each sample, 25ng RNA was hybridised with XT Hs HostResponse CSO code set containing 785 human genes including 12 internal reference genes using Nanostring's nCounter XT Code-Set Gene Expression Assay protocol. After hybridization for 20 h at 65°C, samples were loaded onto an nCounter cartridge and run on the Nanostring nCounter *SPRINT*™ Profiler.

2.5. Data normalisation

The reporter code counts were collected, a quality check of the raw data was performed, followed by normalisation using the nSolver Analysis Software v4.0 (NanoString Technologies, Inc., Seattle, WA, USA). Only reference genes with a raw probe count above 100 were included in the normalisation process. The background threshold was defined as mean + 2 standard deviation (SD) of all negative controls for each sample separately. Samples were normalised by using the sample specific mRNA positive normalisation factor and mRNA content normalisation factor. Genes that had counts under the level of detection and a signal to noise ratio lower than 1 were excluded from the statistical analysis.

2.6. Quantitative polymerase chain reaction (qPCR)

A High-Capacity cDNA Reverse Transcription kit (Applied Biosystems, Paisley, UK) was used to transcribe RNA into cDNA according to the manufacturer's instructions. The cDNA was analysed using Taqman quantitative PCR assays (Life Technologies, Carlsbad, USA) using Taqman PCR master mix 2X (Thermo Fisher Scientific, Waltham, MA, USA). The level of *TNFAIP3* (Hs00234713_m1) and *SARM1* (Hs00248344_m1) were determined relative to the geometric mean of the reference genes *HPRT1* (Hs02800695_m1) and *GAPDH* (Hs02758991_g1). The reactions were performed using an Agilent AriaMX thermocycler (Agilent Technologies, Cheshire, UK) as per manufacturer's instructions. Agilent Aria 1.6 software (Agilent Technologies, Cheshire, UK) was used for the collection and analysis of the data. The expression of the gene of interest (GOI) in the COVID-19 groups is described as the fold induction relative to the average expression of the GOI in HCs, normalised to the reference genes ($2^{-\Delta Ct}$) [23].

2.7. Statistics

Statistical analyses were performed with GraphPad version 8 (GraphPad Software Inc., California, USA) and ClustVis (https://biit.cs.ut.ee/clustvis/) [24]. Hierarchical clustering was calculated using Euclidean distance and average linkage. For comparison of expression between two groups (severe COVID-19 vs HCs; mild COVID-19 vs HCs), multiple t-tests were performed. Differentially expressed genes (DEGs) were determined with a log2 fold change (log2FC) >0.5 and a p value <0.05 which was not corrected for multiple comparison to minimise type 2 error. To compare more than 2 groups, significance was determined using one way ANOVA with Dunnet's multiple comparisons test in case of parametric distributed data or Kruskal-Wallis test with Dunnet's multiple comparisons test in case of non-parametric data.

2.8. Gene ontology (GO) and pathway enrichment analysis

Biological functions, molecular functions, pathway enrichment and protein–protein interaction networks of DEGs were determined using online tools in Search Tool for the Retrieval of Interacting Genes Database (STRING v11.0, https://string-db.org/). For functional enrichment analysis of DEGs, gene ontology terms were used, and pathway enrichment analysis was performed using terms from the Kyoto Encyclopedia of Genes and Genomes (KEGG) database. Input data comprised the list of downregulated and upregulated genes identified in differential expression analysis of participants who experienced severe COVID-19 vs HCs.

3. Results

3.1. Convalescent COVID-19 participants exhibit sustained changes in the steady-state expression of monocyte host response genes

To investigate if steady-state host response gene expression was altered in monocytes of convalescent COVID-19 participants, Nanostring gene expression profiling was performed using the nCounter Human Host Response V1 codeset. Monocytes collected from healthy volunteers prior to the emergence of SARS-CoV-2 were used as the HC samples and compared to cells from participants 3–6 months after they experienced mild or severe COVID-19.

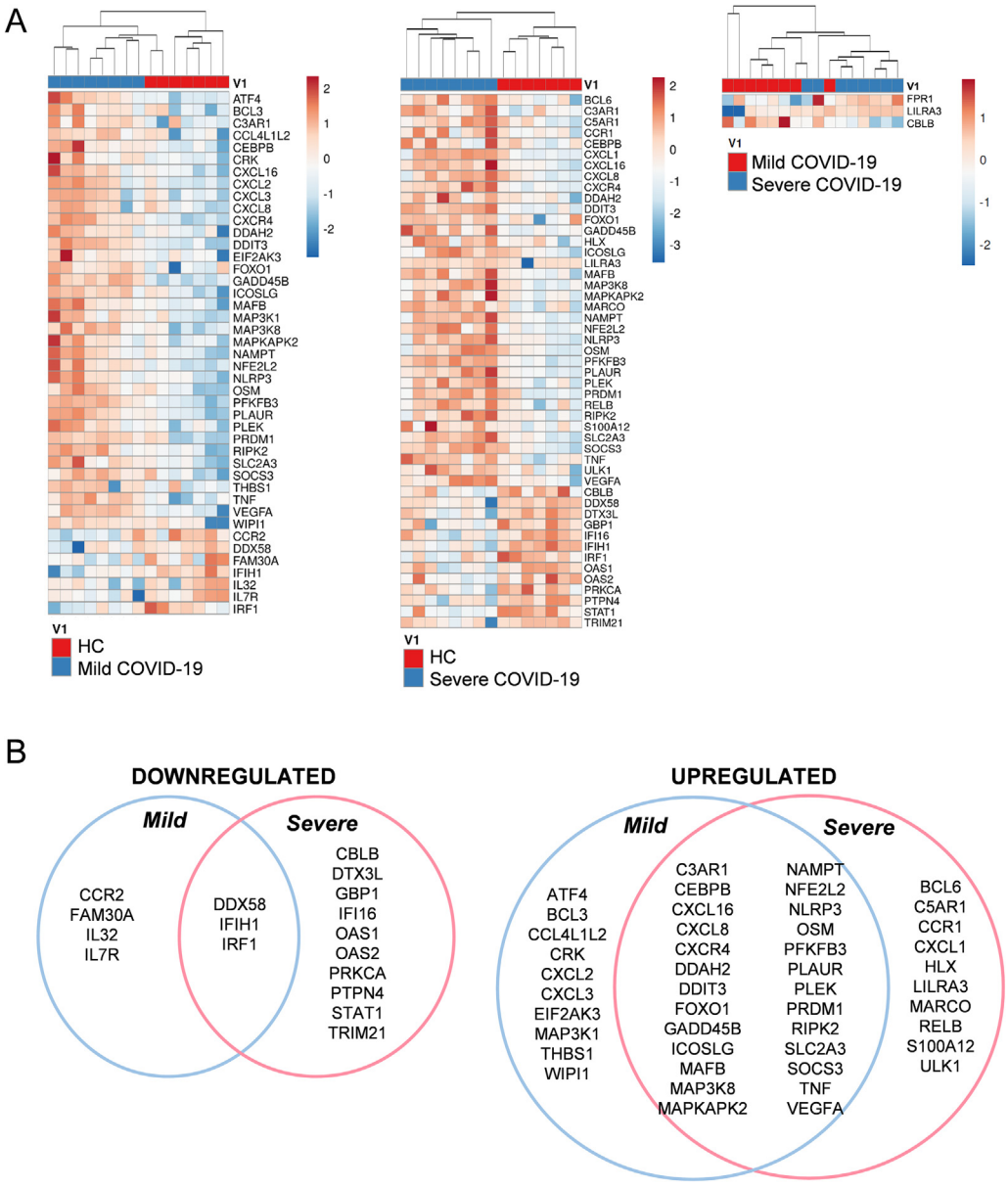

Fig. 1. Differential gene expression analysis of COVID-19 participants and healthy controls (HC). (A) Heatmaps show hierarchical clustering using Euclidean distance and average linkage of DEGs in mild COVID-19 participants vs HCs (left), severe COVID-19 participants vs HCs (middle) and severe vs mild COVID-19 participants (right). Ln(x + 1) transformed data were used to prepare heatmaps with https://biit.cs.ut.ee/clustvis/ (https://doi.org/10.1093/nar/gkv468). (C) Venn diagrams are shown to present shared downregulated (left) and upregulated (right) genes between COVID-19 participants with mild and severe symptoms.

After normalisation and exclusion of genes with low-level counts, 467 of 785 genes were included in the differential gene expression analysis revealing altered expression of several host response genes. Compared to HCs, 36 genes were upregulated and 7 genes were downregulated in the mild COVID-19 group (Fig. 1A, Table S1). In the severe COVID-19 group, 36 genes were upregulated and 13 genes were downregulated (Fig. 1A, Table S2). Further comparison between the mild and severe COVID-19 groups revealed that the genes which encode for the leukocyte immunoglobulin like receptor A3 (*LILRA3*) and the formyl peptide receptor 1 (*FPR1*) were significantly upregulated, and the cbl proto-oncogene B (*CBLB*) was significantly downregulated in the severe COVID-19 group (Fig. 1A, Table S3). When presented in a heatmap showing ln(x + 1) transformed data, the mild COVID-19 group and HCs cluster separately, apart from two of the HCs which clustered with the mild COVID-19 group (Fig. 1A). However, a clear separation of the groups was observed when comparing severe cases with HCs (Fig. 1A). The mild and severe cases formed a separate cluster according to their group classification apart from one case from each group which clustered within the opposite group. In addition, two of the mild COVID-19 participants clustered separately from the two groups (Fig. 1A). When comparing the differential gene expression analysis for each of the COVID-19 groups compared to HCs, there were 26 upregulated genes and 3 downregulated genes that were common to both groups (Fig. 1B).

To confirm that the differential gene expression observed was not due to the slightly lower age of the HC group (Table 1), gene expression was correlated with age in the HC samples for the three genes that were most upregulated in both mild and severe COVID-19 and the three genes that were downregulated in both groups. No correlation was observed between expression of *PFKB3*, *PRDM1*, *OSM*, *DDX58*, *IFIH1* or *IRF1* and age (Fig. S1).

Table 2
The 20 most significantly enriched KEGG pathways of the differentially expressed genes from severe COVID-19 participants compared to healthy controls.

Term ID	Pathway term description	Strength	False discovery rate	Matching proteins in network
		UPREGULATED		
hsa04060	Cytokine-cytokine receptor interaction	1,23	0,00001	OSM, CXCL16, CCR1, CXCL8, CXCL1, CXCR4, TNF, VEGFA
hsa04010	MAPK signaling pathway	1,13	0,00003	GADD45B, RELB, MAP3K8, MAPKAPK2, TNF, DDIT3, VEGFA
hsa04621	NOD-like receptor signaling pathway	1,31	0,00003	RIPK2, NAMPT, CXCL8, NLRP3,CXCL1,TNF
hsa05202	Transcriptional misregulation in cancer	1,3	0,00003	GADD45B, CEBPB, CXCL8, FOXO1, BCL6, DDIT3
hsa04668	TNF signaling pathway	1,41	0,00004	MAP3K8, CEBPB, SOCS3, CXCL1, TNF
hsa04062	Chemokine signaling pathway	1,19	0,00035	CXCL16, CCR1, CXCL8, CXCL1, CXCR4
hsa04064	NF-kappa B signaling pathway	1,38	0,00035	GADD45B, RELB, CXCL8, TNF
hsa04657	IL-17 signaling pathway	1,39	0,00035	CEBPB, CXCL8, CXCL1, TNF
hsa04933	AGE-RAGE signaling pathway in diabetic complications	1,36	0,00035	CXCL8, FOXO1, TNF, VEGFA
hsa05167	Kaposi's sarcoma-associated herpesvirus infection	1,18	0,00035	CCR1, CXCL8, MAPKAPK2, CXCL1, VEGFA
hsa05323	Rheumatoid arthritis	1,43	0,00035	CXCL8, CXCL1, TNF, VEGFA
hsa04932	Non-alcoholic fatty liver disease (NAFLD)	1,18	0,00140	CXCL8, SOCS3, TNF, DDIT3
hsa05134	Legionellosis	1,49	0,00140	CXCL8, CXCL1, TNF
hsa04218	Cellular senescence	1,16	0,00150	GADD45B, CXCL8, MAPKAPK2, FOXO1
hsa05164	Influenza A	1,12	0,00190	CXCL8, SOCS3, NLRP3, TNF
hsa05200	Pathways in cancer	0,81	0,00210	GADD45B, CXCL8, FOXO1, NFE2L2, CXCR4, VEGFA
hsa05133	Pertussis	1,36	0,00240	CXCL8, NLRP3, TNF
hsa04610	Complement and coagulation cascades	1,33	0,00260	C3AR1, PLAUR, C5AR1
hsa05146	Amoebiasis	1,25	0,00420	CXCL8, CXCL1, TNF
hsa04620	Toll-like receptor signaling pathway	1,22	0,00500	MAP3K8, CXCL8, TNF
		DOWNREGULATED		
hsa05162	Measles	1,83	< 0.000001	IFIH1, CBLB, OAS2, STAT1, DDX58, OAS1
hsa05164	Influenza A	1,73	< 0.000001	IFIH1, OAS2, STAT1, DDX58, OAS1, PRKCA
hsa05160	Hepatitis C	1,76	< 0.000001	IRF1, OAS2, STAT1, DDX58, OAS1
hsa04621	NOD-like receptor signaling pathway	1,66	< 0.000001	OAS2, STAT1, IFI16, GBP1, OAS1
hsa05168	Herpes simplex infection	1,62	< 0.000001	IFIH1, OAS2, STAT1, DDX58, OAS1
hsa05161	Hepatitis B	1,63	0,00003	IFIH1, STAT1, DDX58, PRKCA
hsa04622	RIG-I-like receptor signaling pathway	1,63	0,01300	IFIH1, DDX58
hsa04917	Prolactin signaling pathway	1,64	0,01300	IRF1, STAT1
hsa04012	ErbB signaling pathway	1,56	0,01440	CBLB, PRKCA
hsa04933	AGE-RAGE signaling pathway in diabetic complications	1,49	0,01790	STAT1, PRKCA
hsa04919	Thyroid hormone signaling pathway	1,42	0,02210	STAT1, PRKCA

3.2. Pathway and gene ontology analysis of differentially expressed genes in monocytes from the severe COVID-19 group

Functional enrichment analysis was performed on the list of up- and downregulated genes in severe COVID-19 compared to HCs. KEGG pathway analysis revealed that upregulated genes are involved in the cytokine-cytokine receptor interaction pathway (hsa04060), mitogen-activated protein kinase (MAPK) signaling pathway (hsa04010), nucleotide-binding oligomerization domain (NOD)-like signaling pathway (hsa04621), TNF signaling pathway (hsa04668), chemokine signaling pathway (hsa04062) and nuclear factor (NF)-kappa B signaling pathway (hsa04064) along with other immune response pathways (Table 2). GO analysis revealed that the upregulated genes are most significantly enriched in biological processes such as positive regulation of transcription from RNA polymerase II promoter in response to stress (GO:0036003), regulation of alpha–beta T cell differentiation (GO:0046637), positive regulation of leukocyte chemotaxis and migration (GO:0002690, GO:0002687) and positive regulation of MAP kinase activity (GO:0043406) (Table 3). Additionally, upregulated genes are involved in functional molecular processes including protein binding (GO:0005515, GO:0042802), cytokine activity (GO:0005125), signaling receptor binding (GO:0005102) and cytokine receptor binding (GO:0005126) (Table 4).

Downregulated genes were mostly enriched in pathways associated with viral infections such as hepatitis B and C (hsa05161 and hsa05160), measles (hsa05162), influenza A (hsa05164) and also the RIG-I-like-receptor signaling pathway (hsa04622) and NOD-like signaling pathway (hsa04621) (Table 2). These downregulated genes are involved in biological processes associated with interferon production (GO:0060333, GO:0032479, GO:0032481, GO:0032727) and innate anti-viral responses (GO:0051607, GO:0045087) (Table 3). Gene products of downregulated genes function in several binding activities, such as to RNA (GO:0003725, GO:0003723, GO:0003727), DNA (GO:0003690) and enzymes (GO:0019899) (Table 4). To explore the interaction of the proteins derived from the list of DEGs in severe COVID-19, a protein interaction network diagram was constructed with the STRING database. STRING analysis yielded several interacting links between the downregulated (Fig. 2A) and upregulated (Fig. 2B) candidate genes.

3.3. Monocytes from convalescent COVID-19 participants have a reduced response to RIG-I, TLR1/2, and TLR4 activation

As the basal expression of several IFN-related genes, including *DDX58* (the gene encoding for RIG-I) were downregulated in the convalescent COVID-19 group, monocytes were stimulated with 3p-hpRNA to activate RIG-I to explore the functional response. Following stimulation, secretion of CXCL10 was measured as a surrogate marker for the type-I IFN response and was observed to be equivalent across all 3 groups. However, a trend towards a higher constitutive secretion of CXCL10 was observed in the COVID-19 groups, which fell just short of significance in the severe group when compared to the HC monocytes ($p = 0.0569$). Thus, the actual amount of CXCL10 induced by 3p-hpRNA in the COVID-19 monocytes was lower than from the HCs (Fig. 3A). When the induced level of CXCL10 was expressed as the fold change over the constitutive CXCL10 released within each group, there

Table 3
The 20 most significantly enriched functional biological processes of the differentially expressed genes from severe COVID-19 participants compared to healthy controls.

Term ID	Pathway term description	Strength	False discovery rate	Matching proteins in network
		UPREGULATED		
GO:0036003	positive regulation of transcription from RNA polymerase II promoter in response to stress	1,93	<0.000001	CEBPB, NFE2L2, DDIT3, VEGFA
GO:0046637	regulation of alpha–beta T cell differentiation	1,66	<0.000001	RIPK2, NLRP3, HLX, PRDM1, BCL6
GO:0002690	positive regulation of leukocyte chemotaxis	1,57	<0.000001	CCR1, C3AR1, CXCL8, C5AR1, CXCL1, VEGFA
GO:0002687	positive regulation of leukocyte migration	1,49	<0.000001	CCR1, C3AR1, CXCL8, C5AR1, CXCL1, TNF, VEGFA
GO:0030595	leukocyte chemotaxis	1,48	<0.000001	CXCL16, CCR1, CXCL8, C5AR1, S100A12, CXCR4, VEGFA
GO:1902107	positive regulation of leukocyte differentiation	1,45	<0.000001	RIPK2, CCR1, NLRP3, HLX, PRDM1, BCL6, TNF
GO:0060326	cell chemotaxis	1,44	<0.000001	CXCL16,CCR1,C3AR1,CXCL8,C5AR1,S100A12,CXCL1,CXCR4, VEGFA
GO:0050920	regulation of chemotaxis	1,32	<0.000001	CCR1, C3AR1, CXCL8, C5AR1, CXCL1, CXCR4, VEGFA
GO:1902105	regulation of leukocyte differentiation	1,29	<0.000001	RIPK2, CCR1, CEBPB, NLRP3, HLX, PRDM1, MAFB, BCL6, TNF
GO:1903039	positive regulation of leukocyte cell–cell adhesion	1,29	<0.000001	RIPK2, MAP3K8, NLRP3, B7RP1, HLX, BCL6, TNF
GO:0043406	positive regulation of MAP kinase activity	1,28	<0.000001	GADD45B, RIPK2, MAP3K8, C5AR1, MAPKAPK2, S100A12, CXCR4, TNF, VEGFA
GO:0006954	inflammatory response	1,24	<0.000001	RIPK2, RELB, CCR1, C3AR1, CEBPB, CXCL8, NLRP3, C5AR1, MAPKAPK2, S100A12, CXCL1, NFE2L2, BCL6, CXCR4, TNF
GO:0050900	leukocyte migration	1,23	<0.000001	CXCL16, CCR1, C3AR1, CXCL8, C5AR1, S100A12, CXCR4, TNF, VEGFA
GO:1903037	regulation of leukocyte cell–cell adhesion	1,21	<0.000001	RIPK2, MAP3K8, CEBPB, NLRP3, B7RP1, HLX, BCL6, TNF
GO:0032496	response to lipopolysaccharide	1,18	<0.000001	RIPK2, CEBPB, CXCL8, NLRP3, C5AR1, MAPKAPK2, CXCL1, TNF
GO:0050863	regulation of T cell activation	1,17	<0.000001	RIPK2, MAP3K8, CEBPB, NLRP3, B7RP1, HLX, PRDM1, BCL6
GO:0032103	positive regulation of response to external stimulus	1,16	<0.000001	OSM, RIPK2, RELB, CCR1, C3AR1, CXCL8, MARCO, C5AR1, MAPKAPK2, S100A12, CXCL1, TNF, VEGFA
GO:0050867	positive regulation of cell activation	1,16	<0.000001	RIPK2, PLEK, MAP3K8, NLRP3, B7RP1, HLX, PRDM1, BCL6
GO:1903706	regulation of hemopoiesis	1,13	<0.000001	RIPK2, CCR1, CEBPB, NLRP3, HLX, PRDM1, MAFB, NFE2L2, BCL6, TNF
GO:0043410	positive regulation of MAPK cascade	1,12	<0.000001	GADD45B, OSM, RIPK2, MAP3K8, CCR1, MARCO, C5AR1, MAPKAPK2, S100A12, CXCR4, TNF, VEGFA
GO:0050727	regulation of inflammatory response	1,12	<0.000001	OSM, C3AR1, SOCS3, NLRP3, C5AR1, S100A12, BCL6, TNF
		DOWNREGULATED		
GO:0051607	defense response to virus	1,87	<0.000001	IRF1, IFIH1, DTX3L, OAS2, STAT1, IFI16, GBP1, DDX58, OAS1
GO:0045087	innate immune response	1,35	<0.000001	IRF1, TRIM21, IFIH1, DTX3L, OAS2, STAT1, IFI16, GBP1, DDX58, OAS1
GO:0060333	interferon-gamma-mediated signaling pathway	2,12	<0.000001	IRF1, TRIM21, OAS2, STAT1, GBP1, OAS1
GO:0043900	regulation of multi-organism process	1,32	<0.000001	IRF1, TRIM21, IFIH1, DTX3L, STAT1, IFI16, DDX58, OAS1, PRKCA
GO:0032479	regulation of type I interferon production	1,91	<0.000001	IRF1, TRIM21, IFIH1, STAT1, IFI16, DDX58
GO:0032481	positive regulation of type I interferon production	2,06	<0.000001	IRF1, IFIH1, STAT1, IFI16, DDX58
GO:0009605	response to external stimulus	0,89	<0.000001	IRF1, TRIM21, IFIH1, DTX3L, OAS2, STAT1, IFI16, GBP1, DDX58, OAS1, PRKCA
GO:0002831	regulation of response to biotic stimulus	1,39	<0.000001	IRF1, IFIH1, DTX3L, STAT1, IFI16, DDX58, PRKCA
GO:0001817	regulation of cytokine production	1,23	<0.000001	IRF1, TRIM21, IFIH1, STAT1, IFI16, GBP1, DDX58
GO:0034097	response to cytokine	1,07	<0.000001	IRF1, TRIM21, PTPN4, OAS2, STAT1, GBP1, OAS1, PRKCA
GO:0060337	type I interferon signaling pathway	1,97	<0.000001	IRF1, OAS2, STAT1, OAS1
GO:0006950	response to stress	0,7	0,00001	IRF1, TRIM21, IFIH1, DTX3L, OAS2, STAT1, IFI16, GBP1, DDX58, OAS1, PRKCA
GO:0051704	multi-organism process	0,78	0,00001	IRF1, TRIM21, IFIH1, DTX3L, OAS2, STAT1, IFI16, GBP1, DDX58, OAS1
GO:0051716	cellular response to stimulus	0,5	0,00001	IRF1, TRIM21, IFIH1, PTPN4, CBLB, DTX3L, OAS2, STAT1, IFI16, GBP1, DDX58, OAS1, PRKCA
GO:0048525	negative regulation of viral process	1,81	0,00001	TRIM21, STAT1, IFI16, OAS1
GO:0032727	positive regulation of interferon-alpha production	2,29	0,00002	IFIH1, STAT1, DDX58
GO:0002682	regulation of immune system process	0,94	0,00002	IRF1, IFIH1, DTX3L, STAT1, IFI16, GBP1, DDX58, PRKCA
GO:0010033	response to organic substance	0,73	0,00002	IRF1, TRIM21, IFIH1, PTPN4, OAS2, STAT1, GBP1, DDX58, OAS1, PRKCA
GO:0002230	positive regulation of defense response to virus by host	2,24	0,00002	DTX3L, STAT1, DDX58
GO:0032101	regulation of response to external stimulus	1,04	0,00002	IRF1, IFIH1, DTX3L, STAT1, IFI16, DDX58, PRKCA
GO:0071345	cellular response to cytokine stimulus	1,04	0,00002	IRF1, TRIM21, PTPN4, OAS2, STAT1, GBP1, OAS1

was a lower fold increase from the severe COVID-19 monocytes of 2.3 fold, compared to 5.1 fold from the mild COVID-19 monocytes and 19.1 fold from the HC monocytes (Fig. 3A).

To investigate activation of other downstream cytokines, monocytes from convalescent COVID-19 participants and HCs were stimulated with the TLR ligands PAM3 and LPS that activate the TLR1/2 heterodimer and TLR4, respectively. A trend towards lower cytokine production with increasing disease severity was observed following activation with both ligands (Fig. 3B-C). Monocytes from both the mild and severe disease groups, secreted significantly less IL-1β upon stimulation with PAM3 and LPS (Fig. 3B-C). Similarly, LPS induced lower levels of TNF in both the mild and the severe group (Fig. 3C). Addi-

Table 4
The 20 most significantly enriched functional molecular processes of the differentially expressed genes from severe COVID-19 participants compared to healthy controls.

Term ID	Term description	Strength	False discovery rate	Matching proteins in network
			UPREGULATED	
GO:0005515	protein binding	0,37	0,00001	OSM, RIPK2, RELB, NAMPT, PLEK, CXCL16, CCR1, CEBPB, CXCL8, MARCO, ULK1, SOCS3, NLRP3, PLAUR, B7RP1, C5AR1, MAPKAPK2, S100A12, PRDM1, MAFB, FOXO1, CXCL1, NFE2L2, BCL6, CXCR4, TNF, DDIT3, VEGFA
GO:0005125	cytokine activity	1,26	0,00001	OSM, NAMPT, CXCL16, CXCL8, CXCL1, TNF, VEGFA
GO:0005102	signaling receptor binding	0,68	0,00008	OSM, RIPK2, NAMPT, CXCL16, CEBPB, CXCL8, MARCO, PLAUR, B7RP1, S100A12, CXCL1, TNF, VEGFA
GO:0042802	identical protein binding	0,62	0,00032	RIPK2, RELB, NAMPT, PLEK, CEBPB, ULK1, NLRP3, B7RP1, MAFB, BCL6, TNF, DDIT3, VEGFA
GO:0005488	binding	0,19	0,00033	SLC2A3, OSM, RIPK2, RELB, NAMPT, PLEK, MAP3K8, CXCL16, CCR1, CEBPB, CXCL8, MARCO, ULK1, SOCS3, NLRP3, PLAUR, B7RP1, C5AR1, HLX, MAPKAPK2, S100A12, PRDM1, MAFB, DDAH2, FOXO1, CXCL1, NFE2L2, BCL6, CXCR4, TNF, PFKFB3, DDIT3, VEGFA
GO:0005126	cytokine receptor binding	1,09	0,00034	OSM, CXCL16, CXCL8, CXCL1, TNF, VEGFA
GO:0043565	sequence-specific DNA binding	0,73	0,00035	RELB, CEBPB, NLRP3, HLX, PRDM1, MAFB, FOXO1, NFE2L2, BCL6, DDIT3
GO:0000976	transcription regulatory region sequence-specific DNA binding	0,73	0,00210	RELB, CEBPB, PRDM1, MAFB, NFE2L2, BCL6, TNF, DDIT3
GO:0008009	chemokine activity	1,54	0,00210	CXCL16, CXCL8, CXCL1
GO:0000977	RNA polymerase II transcription regulatory region sequence-specific DNA binding	0,78	0,00240	RELB, CEBPB, PRDM1, MAFB, NFE2L2, BCL6, DDIT3
GO:0004875	complement receptor activity	2,05	0,00330	C3AR1, C5AR1
GO:0000978	RNA polymerase II proximal promoter sequence-specific DNA binding	0,83	0,00340	RELB, CEBPB, PRDM1, MAFB, NFE2L2, DDIT3
GO:0019957	C-C chemokine binding	2,01	0,00340	CCR1, CXCR4
GO:0000981	DNA-binding transcription factor activity, RNA polymerase II-specific	0,53	0,00500	RELB, PLEK, CEBPB, HLX, PRDM1, MAFB, FOXO1, NFE2L2, BCL6, DDIT3
GO:0045236	CXCR chemokine receptor binding	1,84	0,00510	CXCL8, CXCL1
GO:0042803	protein homodimerization activity	0,67	0,00620	RIPK2, NAMPT, PLEK, CEBPB, MAFB, DDIT3, VEGFA
GO:0008134	transcription factor binding	0,74	0,00680	CEBPB, NLRP3, MAFB, FOXO1, NFE2L2, DDIT3
GO:0001227	DNA-binding transcription repressor activity, RNA polymerase II-specific	0,99	0,00690	CEBPB, PRDM1, FOXO1, BCL6
GO:0019899	enzyme binding	0,45	0,00950	RIPK2, RELB, PLEK, CEBPB, ULK1, PLAUR, MAPKAPK2, PRDM1, FOXO1, CXCR4, TNF
GO:0004950	chemokine receptor activity	1,62	0,00980	CCR1, CXCR4
			DOWNREGULATED	
GO:0003725	double-stranded RNA binding	1,93	0,00002	IFIH1, OAS2, DDX58, OAS1
GO:0001730	2′-5′-oligoadenylate synthetase activity	3	0,00028	OAS2, OAS1
GO:0003723	RNA binding	0,95	0,00530	TRIM21, IFIH1, OAS2, DDX58, OAS1
GO:0008270	zinc ion binding	0,97	0,00530	TRIM21, IFIH1, CBLB, DDX58, PRKCA
GO:0097159	organic cyclic compound binding	0,45	0,00620	IRF1, TRIM21, IFIH1, OAS2, STAT1, IFI16, GBP1, DDX58, OAS1, PRKCA
GO:1901363	heterocyclic compound binding	0,45	0,00620	IRF1, TRIM21, IFIH1, OAS2, STAT1, IFI16, GBP1, DDX58, OAS1, PRKCA
GO:0003676	nucleic acid binding	0,56	0,00710	IRF1, TRIM21, IFIH1, OAS2, STAT1, IFI16, DDX58, OAS1
GO:0003824	catalytic activity	0,43	0,00710	TRIM21, IFIH1, PTPN4, CBLB, DTX3L, OAS2, GBP1, DDX58, OAS1, PRKCA
GO:0035639	purine ribonucleoside triphosphate binding	0,7	0,00710	IFIH1, OAS2, GBP1, DDX58, OAS1, PRKCA
GO:0042802	identical protein binding	0,71	0,00710	TRIM21, IFIH1, STAT1, IFI16, GBP1, DDX58
GO:0032555	purine ribonucleotide binding	0,69	0,00750	IFIH1, OAS2, GBP1, DDX58, OAS1, PRKCA
GO:0044389	ubiquitin-like protein ligase binding	1,14	0,01030	DTX3L, STAT1, DDX58
GO:0003690	double-stranded DNA binding	0,86	0,01080	IRF1, STAT1, IFI16, DDX58
GO:0003727	single-stranded RNA binding	1,58	0,01080	IFIH1, DDX58
GO:0004842	ubiquitin-protein transferase activity	1,09	0,01080	TRIM21, CBLB, DTX3L
GO:0005488	binding	0,22	0,01080	IRF1, TRIM21, IFIH1, PTPN4, CBLB, DTX3L, OAS2, STAT1, IFI16, GBP1, DDX58, OAS1, PRKCA
GO:0005515	protein binding	0,36	0,01080	TRIM21, IFIH1, PTPN4, CBLB, DTX3L, STAT1, IFI16, GBP1, DDX58, PRKCA
GO:0005524	ATP binding	0,71	0,01080	IFIH1, OAS2, DDX58, OAS1, PRKCA
GO:0016740	transferase activity	0,6	0,01080	TRIM21, CBLB, DTX3L, OAS2, OAS1, PRKCA
GO:0019899	enzyme binding	0,61	0,01080	CBLB, DTX3L, STAT1, GBP1, DDX58, PRKCA

tionally, monocytes from the severe COVID-19 group secreted significantly lower levels of IL-6 following stimulation with PAM3 and LPS (Fig. 3B-C).

3.4. Steady-state expression of SOCS3 and SIGIRR are increased in convalescent COVID-19 monocytes

Signaling downstream of TLRs is controlled by proteins that become upregulated following TLR activation to negatively regulate and terminate signaling [25]. Several signaling regulators were included on the nanostring panel, of which suppressor of cytokine signaling (*SOCS)3* and single Ig IL-1-related receptor (*SIGIRR*) were significantly upregulated in monocytes of the convalescent COVID-19 group (Fig. 4A) [26,27]. However, other negative regulators of the TLR downstream signaling cascade, interleukin-1 receptor-associated kinase (*IRAK*) 3 and toll interacting protein (*TOLLIP*), showed no difference in expression between the groups (Fig. 4A) [28,29]. The expression of two other GOIs, which were measured separately by

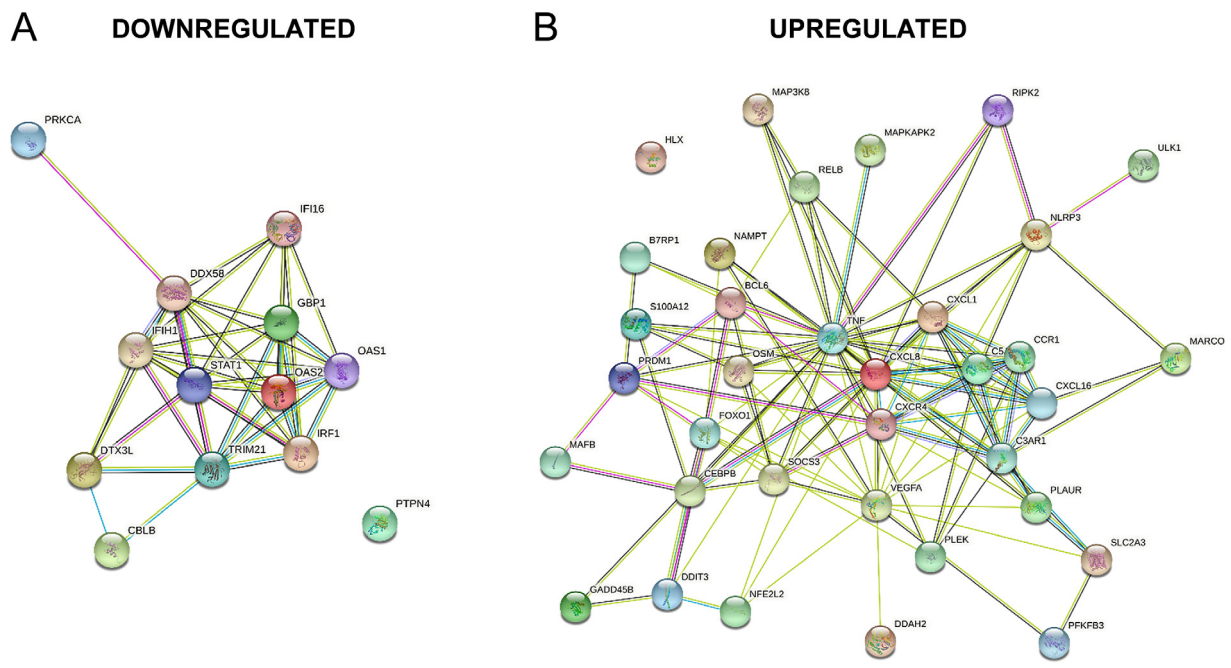

Fig. 2. Protein interaction analysis of differentially expressed genes from severe COVID-19 participants. Interaction network of (A) downregulated and (B) upregulated genes from severe COVID-19 participants compared to HCs. Network nodes represent proteins. Edges represent protein–protein associates. The line colors represent the type of evidence used in predicting associations (known interactions derived from curated databases: cyan; experimental evidence: pink; text mining: yellow; co-expression: black; protein homology: light blue) Analysis was performed with the STRING database version 11.0 (https://string-db.org/).

qPCR as they were not on the nanostring panel, were also comparable across the groups. These included the sterile α and HEAT/Armadillo motif containing protein 1 (*SARM1*), a negative regulator of the NOD-like receptor family pyrin domain containing (NLRP)3 inflammasome (a suppressor of IL-1β maturation), and *TNFAIP3,* the gene encoding the TNF-alpha-induced protein 3 (a negative regulator of the canonical NF-κB signaling pathway) (Fig. 4B) [30,31].

4. Discussion

Following infection with SARS-CoV-2, monocytes undergo remodelling of chromatin accessibility, suggesting an extended period of trained immunity [6,7]. Interestingly, a similar effect occurs following vaccination against SARS-CoV-2, where a reduction in chromatin accessibility has been observed for several inflammatory genes [32]. Although monocytes are short-lived in the periphery, sustained changes can be introduced through central trained immunity of hematopoietic stem cells and bone marrow progenitor cells, a phenomenon first observed after BCG vaccination [33]. Immune training following COVID-19, could alter steady-state gene expression *in vivo*, potentially modifying cellular activation thresholds and consequently the inflammatory response to subsequent stimulation. In support of this concept, the present study has identified several differentially expressed host response genes in steady-state monocytes 3–6 months following infection with SARS-CoV-2, alongside tolerance to innate immune receptor activation.

The upregulated genes were positively associated with regulation of leukocyte chemotaxis and migration and regulation of MAP kinase activity. Consistent with this data, several of the upregulated genes are supported by other studies of convalescent COVID-19 patients. For example, *CXCL8* is upregulated in the serum of convalescent COVID-19 patients 4 months post infection [34]. S100 calcium-binding protein A12 (S100A12) and oncostatin m (OSM) are upregulated in plasma during the first 30 days of SARS-COV-2 infection and in serum from convalescent COVID-19 patients 7–8 months post infection [35,36]. Consequently, it might be expected that upon activation of TLR2 and TLR4 that respond to the SARS-CoV-2 envelope protein and the spike protein S1 subunit respectively, an amplified response may be observed in the convalescent COVID-19 samples [12,14,15]. However, monocytes from both convalescent COVID-19 groups exhibited a reduced response to TLR1/2 and TLR4 stimulation resulting in lower secretion of IL-1β, IL-6 and TNF.

Supporting this observation, activation of TLR2 by the SARS-CoV-2 envelope protein has recently been shown to induce innate immune tolerance to subsequent stimulation with LPS 6 days later in human monocytes and in a murine LPS challenge model [37]. In addition, a reduced TLR4 response following COVID-19 infection has previously been reported at several earlier time points in the recovery period. In mild and severe COVID-19 patients, decreased monocyte IL-1β and TNF secretion in response to LPS has been observed between day 4 and 13 post symptom onset [38]. Moreover, this effect is also reported 2–4 weeks after disease onset, where convalescent COVID-19 monocytes produced lower levels of TNF and IL-6 following LPS stimulation [39]. Our data now suggest that this reduction in TLR4 induced cytokines extends beyond the first few weeks post infection, potentially lasting for several months. Interestingly, a similar decrease in TLR4-induced TNF has also been observed in monocytes 15–150 days following COVID-19 vaccination with both inactivated vaccines and non-replicating viral vector vaccines [32]. Conversely, a study of LPS activated monocytes collected from convalescent COVID-19 patients 6 months after infection indicated no change in IL-1β, TNF or IL-6, with only a reduction in CXCL10 compared to unvaccinated HCs [7]. This may indicate that the suppression of the TLR4 response via the myeloid differentiation primary response protein 88 (MyD88) signalling pathway is not sustained beyond 6 months post infection.

The downregulated genes identified by the nanostring panel were mainly associated with the regulation of IFN and innate anti-viral responses. Downregulation of *IRF1*, *IFIH1* and *DDX58* were common to both the mild and severe COVID-19 samples compared to HCs. Interestingly, *IFIH1* and *DDX58* encode for the receptors MDA5 and RIG-I which are sensors of viral RNA motifs that induce a type-I IFN response and can both be activated by SARS-CoV-2 [10,40,41]. Expres-

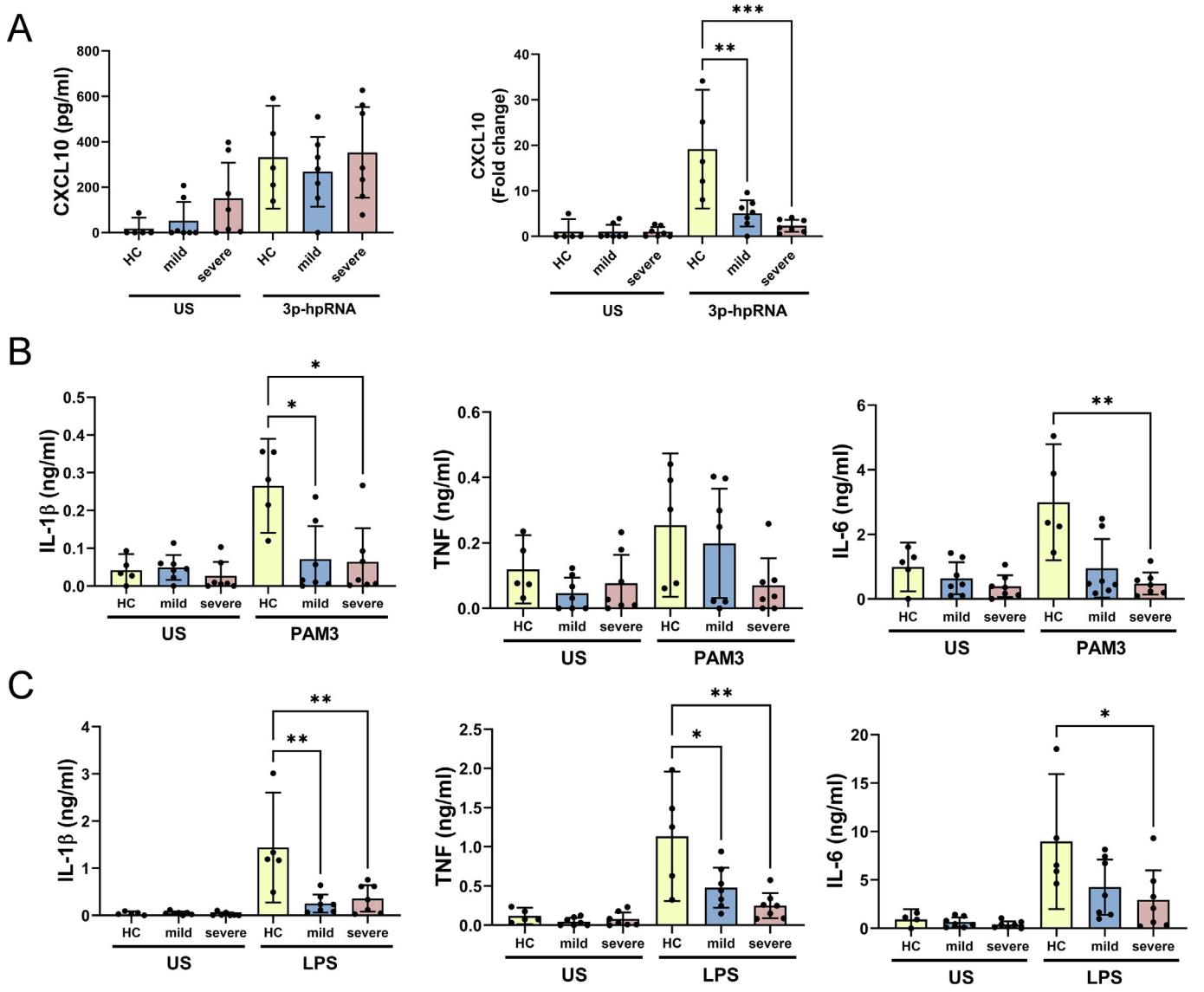

Fig. 3. Monocytes from convalescent COVID-19 participants exhibit a lowered cytokine response upon activation. Primary human monocytes were unstimulated (US) or stimulated for 24 h with 1 μg/ml 3p-hpRNA, 100 ng/ml Pam3, or 10 ng/ml LPS. (A) CXCL10, (B, C) IL-1β, IL-6 and TNF secretion were measured by ELISA. (A-C) Data are displayed as pooled data as mean ± 95 % CI from 5 to 8 healthy controls (HC), 7–8 mild COVID-19 participants and 7 severe COVID-19 participants. (A) The CXCL10 data is also displayed as the fold change compared to the corresponding US control and presented as the as mean ± 95 % CI. (A-C) Significance was determined using a one-way ANOVA with Dunnet's multiple comparisons test or a Kruskal-Wallis test with Dunnet's multiple comparisons test (*$p \leq 0.05$, **$p \leq 0.01$, ***$p \leq 0.001$).

sion of *STAT1,* the IFN inducible antiviral proteins oligoadenylate synthetase (*OAS)1*, *OAS2,* and interferon-γ-inducible (*IFI)16* that recognizes dsDNA to induce type-I IFN were also decreased in the severe group. *STAT1* is important for the early responses to IFNs, with STAT1 deficiency also associated with suppression of TLR2 and TLR4 responses in murine peritoneal macrophages [42,43]. Notably, *OAS1* is suggested to influence the severity of COVID-19 and *IFI16* has a role in maintaining latency of Epstein Barr Virus (EBV), which has been observed to become reactivated following severe COVID-19 [44].

IFNs are the cornerstone of the antiviral immune response. Thus, a delayed or an impaired IFN response due to reduced or no expression of crucial genes involved in the IFN pathways can have detrimental effects. This was demonstrated in COVID-19 where mutations in genes involved in the regulation of type I and III IFNs were associated with severe disease [45]. Compounding this, advanced age, which is a risk factor for severe COVID-19, is also associated with an impaired IFN response, with reduced monocyte/dendritic cell recruitment and activation resulting in reduced T and B cell activation and higher viral load [46]. However, a reduced IFN response upon reinfection with SARS-CoV-2 in convalescent COVID-19 may not be as detrimental due to the presence of adaptive immune memory following the initial infection.

Curiously, monocytes from several of the COVID-19 participants spontaneously produced CXCL10 when cultured, most notably in the severe group. Similarly elevated serum CXCL10 levels have been reported in convalescent COVID-19 patients 4 months after the initial infection [34]. The reason for the spontaneous release was unclear. Upon stimulation of RIG-I, the overall levels of CXCL10 released were similar across the groups, however, due to the different background levels of spontaneous CXCL10 release, this represented a reduced induction of CXCL10 in response to RIG-I activation in the monocytes from the COVID-19 participants compared to the HCs, with the lowest

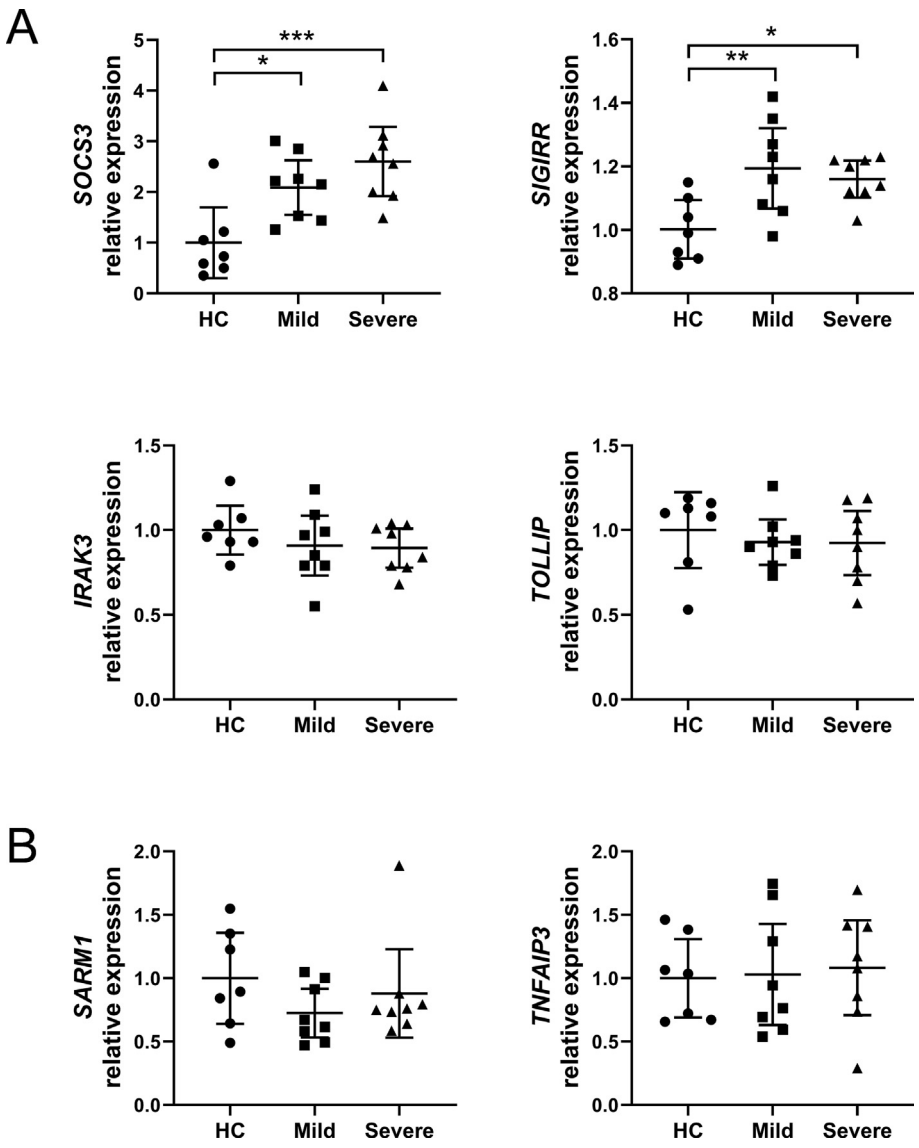

Fig. 4. The steady-state expression of the negative regulators *SOCS3* and *SIGIRR* is increased in monocytes from convalescent COVID-19 participants. Plots show relative steady-state expression of (A) *SOCS3, SIGIRR, IRAK3, TOLLIP,* (B) *SARM1* and *TNFAIP3* in monocytes derived from convalescent COVID-19 participants experiencing mild or severe symptoms (each group n = 8) compared to healthy controls (HC) (n = 7). (A, B) The data are displayed as the mean ± 95 % CI. Significance was determined using a one-way ANOVA with Dunnet's multiple comparisons test or a Kruskal-Wallis test with Dunnet's multiple comparisons test (*p ≤ 0.05, ** p ≤ 0.01, ***p ≤ 0.001).

fold induction of CXCL10 in monocytes from the severe COVID-19 group. This suggests that monocytes may exhibit a moderated response to RIG-I activation during recovery from COVID-19.

A potential explanation for the decreased cytokine production following RIG-I, TLR2 and TLR4 activation might be decreased *STAT1* expression, which can lead to suppression of TLR activation, lower receptor expression, or could be due to increased negative regulation of the downstream signaling cascades, similar to the mechanism underlying endotoxin tolerance [42,47,48]. Several signaling regulators were included on the nanostring panel of which *SOCS3* and *SIGIRR* were both upregulated following COVID-19. Interestingly, upregulation of *SOCS3* has also been observed in monocytes during the first few weeks following SARS-CoV-2 infection [49]. SOCS3 is best known as an inhibitor of the janus kinase (JAK)-signal transducer and activator of transcription (STAT) pathway, but has also been suggested to inhibit TNF receptor-associated factor (TRAF) 6 and TGF-β-activated kinase (TAK) 1, both of which are components of the TLR signaling pathway [27]. Likewise, SIGIRR is a negative regulator of TLR signaling, proposed to sequester the proximal signaling molecules TRAF6 and IRAK1 [50]. Nevertheless, further work would be required to determine if the expression of these proteins following cell activation differs from HCs during recovery from COVID-19 and contributes to the tolerogenic responses observed in the present study.

Together the data presented in this study contribute to the growing literature demonstrating the long-term effects of COVID-19 on monocytes. However, there are several limitations within the study. The NanoString nCounter assay restricted the DEG analysis to a predesigned selection of host response genes which may overlook broader transcriptomic changes that could be identified by RNAseq. Furthermore, changes in gene expression identified by the NanoString panel or by qPCR do not always reflect changes in protein, thus further investigation at the protein level would be required in future studies. Additionally, the sample size was small and the HC participants had a slightly lower age to the COVID-19 donors. However, no correlation was observed between age and gene expression in the HC samples, suggesting that age would not influence the DEG observed in the mild

and severe COVID-19 groups, particularly given the severe group were of a similar age to the mild group yet displayed the largest changes in expression and response to innate receptor stimulation.

Overall, the data presented within this study agree with other published studies, suggesting that exposure to SARS-CoV-2 leads to a sustained alteration of host response gene expression post infection. Furthermore, the data reveal tolerance of TLR2, TLR4 and RIG-I activation lasting 3–6 months after SARS-CoV-2 infection in people recovering from both mild and severe COVID-19. As these receptors can each be activated by SARS-CoV-2, this may provide a protective moderated inflammatory response to subsequent reinfection [12,14,15,40]. Inhibition of TLR2 is reported to reduce mortality in a murine model of SARS-COV-2 infection [13]. Conversely this may be less advantageous for vaccination. Indeed, prior infection with SARS-CoV-2 has been observed to reduce CD8+ T cell activation after BNT162b2 vaccination and to decrease B cell responses to a booster vaccine in people who were recently infected [51,52].

A clinical consequence of a sustained decrease in the response of these pattern recognition receptors could also be an increased susceptibility to other bacterial and viral infections. COVID-19 patients have been shown to develop co-infections and superinfections with other pathogens during the early stages of the disease, but less is known about the risk during convalescence [53,54]. An increased risk for streptococcal tonsillitis has been reported up to a year after SARS-CoV-2 infection and an increase in reactivation of latent EBV has also been observed following COVID-19 [44,55]. The innate immune system recognizes pathogens using combinations of pattern recognition receptors to generate an inflammatory response, consequently there is a level of redundancy within the system. Thus, downregulation of the activity of some innate immune receptors but not others may simply adjust the inflammatory response to some infections, rather than deactivating it. Further characterization of how the immune response is modified by SARS-CoV-2 and a better understanding of the effect this has on innate immune cell function will be needed to determine whether these mechanisms form part of a detrimental or protective host response to subsequent infections.

CRediT authorship contribution statement

Sarah Unterberger: Writing – review & editing, Writing – original draft, Methodology, Investigation, Formal analysis, Data curation, Conceptualization. **Nadia Terrazzini:** Writing – review & editing, Investigation, Formal analysis. **Sandra Sacre:** Writing – review & editing, Writing – original draft, Supervision, Project administration, Methodology, Funding acquisition, Formal analysis, Data curation, Conceptualization.

Funding

This work was funded by the University of Brighton, Brighton and Sussex Medical School and a Nanostring nCounter Host Response panel grant.

Data availability statement

The gene expression data that support the findings of this study are openly available in Gene Expression Omnibus (https://www.ncbi.nlm.nih.gov/geo/summary), reference number GSE181958. All other data are contained within the manuscript.

Declaration of competing interest

The authors declare that they have no known competing financial interests or personal relationships that could have appeared to influence the work reported in this paper.

Acknowledgments

We would like to thank Florian Kern, Juliet Kneller, Jose Pacheco Benitez, Aalia Bano and Daire Cantillon for the collection of participant data and the COVID-19 samples held at Brighton and Sussex Medical School.

Appendix A. Supplementary data

Supplementary data to this article can be found online at https://doi.org/10.1016/j.humimm.2025.111249.

References

[1] C. Huang et al, *Clinical features of patients infected with 2019 novel coronavirus in Wuhan, China.* the Lancet 395 (10223) (2020) 497–506.
[2] W.-J. Guan et al, *Clinical Characteristics of Coronavirus Disease 2019 in China*, N. Engl. J. Med. 382 (18) (2020) 1708–1720.
[3] C. Qin et al, *Dysregulation of Immune Response in Patients With Coronavirus 2019 (COVID-19) in Wuhan, China*, Clin. Infect. Dis. 71 (15) (2020) 762–768.
[4] T. Greenhalgh et al, *Long COVID: a clinical update*, Lancet 404 (10453) (2024) 707–724.
[5] A.D. Proal et al, *SARS-CoV-2 reservoir in post-acute sequelae of COVID-19 (PASC)*, Nat. Immunol. 24 (10) (2023) 1616–1627.
[6] M. You et al, *Single-cell epigenomic landscape of peripheral immune cells reveals establishment of trained immunity in individuals convalescing from COVID-19*, Nat. Cell Biol. 23 (6) (2021) 620–630.
[7] A. Utrero-Rico et al, *Alterations in Circulating Monocytes Predict COVID-19 Severity and Include Chromatin Modifications Still Detectable Six Months after Recovery*, Biomedicines 9 (9) (2021).
[8] J.-G. Cheong et al, *Epigenetic memory of coronavirus infection in innate immune cells and their progenitors*, Cell 186 (18) (2023) 3882–3902.e24.
[9] V. Salvi et al, *SARS-CoV-2–associated ssRNAs activate inflammation and immunity via TLR7/8*, JCI Insight 6 (18) (2021).
[10] N.G. Sampaio et al, *The RNA sensor MDA5 detects SARS-CoV-2 infection*, Sci. Rep. 11 (1) (2021) 13638.
[11] T. Kouwaki et al, *RIG-I-Like Receptor-Mediated Recognition of Viral Genomic RNA of Severe Acute Respiratory Syndrome Coronavirus-2 and Viral Escape From the Host Innate Immune Responses*, Front. Immunol. 12 (2021).
[12] R. Planès et al, *SARS-CoV-2 Envelope (E) Protein Binds and Activates TLR2 Pathway: A Novel Molecular Target for COVID-19 Interventions*, Viruses 14 (5) (2022).
[13] M. Zheng et al, *TLR2 senses the SARS-CoV-2 envelope protein to produce inflammatory cytokines*, Nat. Immunol. 22 (2021) 829–838.
[14] K. Shirato, T. Kizaki, *SARS-CoV-2 spike protein S1 subunit induces pro-inflammatory responses via toll-like receptor 4 signaling in murine and human macrophages*, Heliyon 7 (2021).
[15] Y. Zhao et al, *Publisher Correction: SARS-CoV-2 spike protein interacts with and activates TLR4*, Cell Res. 31 (2020) 825.
[16] E.R. Mann et al, *Longitudinal immune profiling reveals key myeloid signatures associated with COVID-19*, Sci. Immunol. 5 (51) (2020) eabd6197.
[17] Y. Zhou et al, *Pathogenic T-cells and inflammatory monocytes incite inflammatory storms in severe COVID-19 patients*, Natl. Sci. Rev. 7 (6) (2020) 998–1002.
[18] H.W. Löms Ziegler-Heitbrock, M. Frankenberger, A. Wedel, *Tolerance to Lipopolysaccharide in Human Blood Monocytes*, Immunobiology 193 (2) (1995) 217–223.
[19] S. Sato et al, *Synergy and Cross-Tolerance Between Toll-Like Receptor (TLR) 2- and TLR4-Mediated Signaling Pathways*, J. Immunol. 165 (12) (2000) 7096–7101.
[20] M.G. Netea et al, *Defining trained immunity and its role in health and disease*, Nat. Rev. Immunol. 20 (6) (2020) 375–388.
[21] J. Kleinnijenhuis et al, *Bacille Calmette-Guérin induces NOD2-dependent nonspecific protection from reinfection via epigenetic reprogramming of monocytes*, Proc. Natl. Acad. Sci. 109 (43) (2012) 17537–17542.
[22] A. Bøyum, *Separation of Blood Leucocytes, Granulocytes and Lymphocytes*, Tissue Antigens 4 (3) (1974) 269–274.
[23] K.J. Livak, T.D. Schmittgen, *Analysis of Relative Gene Expression Data Using Real-Time Quantitative PCR and the $2-\Delta\Delta CT$ Method*, Methods 25 (4) (2001) 402–408.
[24] T. Metsalu, J. Vilo, *ClustVis: a Web Tool for Visualizing Clustering of Multivariate Data Using Principal Component Analysis and Heatmap* Rheumatology 43 (2015) W566–W570.
[25] T. Kondo, T. Kawai, S. Akira, *Dissecting negative regulation of Toll-like receptor signaling*, Trends Immunol. 33 (9) (2012) 449–458.
[26] D. Wald et al, *SIGIRR, a negative regulator of Toll-like receptor–interleukin 1 receptor signaling*, Nat. Immunol. 4 (9) (2003) 920–927.
[27] H. Frobøse et al, *Suppressor of Cytokine Signaling-3 Inhibits Interleukin-1 Signaling by Targeting the TRAF-6/TAK1 Complex*, Mol. Endocrinol. 20 (7) (2006) 1587–1596.
[28] K. Kobayashi et al, *IRAK-M Is a Negative Regulator of Toll-like Receptor Signaling*, Cell 110 (2) (2002) 191–202.
[29] G. Zhang, S. Ghosh, *Negative Regulation of Toll-like Receptor-mediated Signaling by Tollip **, J. Biol. Chem. 277 (9) (2002) 7059–7065.
[30] R. Pujari et al, *A20-mediated negative regulation of canonical NF-κB signaling pathway*, Immunol. Res. 57 (1) (2013) 166–171.

[31] M. Carty et al, *Cell Survival and Cytokine Release after Inflammasome Activation Is Regulated by the Toll-IL-1R Protein SARM*, Immunity (2019).
[32] M.d.S.M. Antunes et al, *COVID-19 inactivated and non-replicating viral vector vaccines induce regulatory training phenotype in human monocytes under epigenetic control*, Front. Cell. Infect. Microbiol. 13 (2023).
[33] E. Kaufmann et al, *BCG Educates Hematopoietic Stem Cells to Generate Protective Innate Immunity against Tuberculosis*, Cell 172 (1) (2018) 176–190.e19.
[34] C. Phetsouphanh et al, *Immunological dysfunction persists for 8 months following initial mild-to-moderate SARS-CoV-2 infection*, Nat. Immunol. 23 (2) (2022) 210–216.
[35] L. Tserel et al, *Long-Term Elevated Inflammatory Protein Levels in Asymptomatic SARS-CoV-2 Infected Individuals*, Front. Immunol. 12 (2021).
[36] L. Haljasmägi et al, *Longitudinal proteomic profiling reveals increased early inflammation and sustained apoptosis proteins in severe COVID-19*, Sci Rep 10 (1) (2020) 20533.
[37] E.S. Geanes et al, *SARS-CoV-2 envelope protein regulates innate immune tolerance*, iScience 27 (6) (2024) 109975.
[38] J. Schulte-Schrepping et al, *Severe COVID-19 Is Marked by a Dysregulated Myeloid Cell Compartment*, Cell 182 (6) (2020) 1419–1440.e23.
[39] E.V. Ravkov et al, *Reduced monocyte proportions and responsiveness in convalescent COVID-19 patients*, Front. Immunol. 14 (2024).
[40] D.-M. Yang et al, *Differential roles of RIG-I like receptors in SARS-CoV-2 infection*, Mil. Med. Res. 8 (1) (2021) 49.
[41] M. Brisse, H. Ly, *Comparative Structure and Function Analysis of the RIG-I-Like Receptors: RIG-I and MDA5*, Front. Immunol. 10 (1586) (2019).
[42] H.S. Kim et al, *STAT1 deficiency redirects IFN signalling toward suppression of TLR response through a feedback activation of STAT3*, Sci. Rep. 5 (1) (2015) 13414.
[43] X.F. Kong et al, *A novel form of human STAT1 deficiency impairing early but not late responses to interferons*, Blood 116 (26) (2010) 5895–5906.
[44] K.D.E. Bernal, C.B. Whitehurst, *Incidence of Epstein-Barr virus reactivation is elevated in COVID-19 patients*, Virus Res. 334 (2023) 199157.
[45] Q. Zhang et al, *Inborn errors of type I IFN immunity in patients with life-threatening COVID-19*, Science 370 (6515) (2020).
[46] E. Feng et al, *Aging and Interferons: Impacts on Inflammation and Viral Disease Outcomes*. 10 (3) (2021) 708.
[47] Y. Xiong et al, *Endotoxin tolerance impairs IL-1 receptor-associated kinase (IRAK) 4 and TGF-beta-activated kinase 1 activation, K63-linked polyubiquitination and assembly of IRAK1, TNF receptor-associated factor 6, and IkappaB kinase gamma and increases A20 expression*, J. Biol. Chem. 286 (10) (2011) 7905–7916.
[48] C. Munoz et al, *Dysregulation of in vitro cytokine production by monocytes during sepsis*, J. Clin. Invest. 88 (5) (1991) 1747–1754.
[49] W. Wen et al, *Immune cell profiling of COVID-19 patients in the recovery stageby single-cell sequencing*, Cell Discovery 6 (1) (2020) 31.
[50] J. Qin et al, *SIGIRR inhibits interleukin-1 receptor- and toll-like receptor 4-mediated signaling through different mechanisms*, J Biol Chem 280 (26) (2005) 25233–25241.
[51] F. Gao et al, Immunity 56 (4) (2023) 864–878.e4.
[52] C.M. Buckner et al, *Interval between prior SARS-CoV-2 infection and booster vaccination impacts magnitude and quality of antibody and B cell responses*, Cell 185 (23) (2022) 4333–4346.e14.
[53] J.S. Musuuza et al, *Prevalence and outcomes of co-infection and superinfection with SARS-CoV-2 and other pathogens: A systematic review and meta-analysis*, PLoS One 16 (5) (2021) e0251170.
[54] N. Shafran et al, *Secondary bacterial infection in COVID-19 patients is a stronger predictor for death compared to influenza patients*, Sci. Rep. 11 (1) (2021) 12703.
[55] B. Mizrahi et al, *Long covid outcomes at one year after mild SARS-CoV-2 infection: nationwide cohort study*, BMJ 380 (2023) e072529.